Environmental factors controlling the distribution of rhodoliths: An integrated study based on seafloor sampling, ROV and side scan sonar data, offshore the W-Pontine Archipelago

E. Sañé[a],*, F.L. Chiocci[a], D. Basso[b], E. Martorelli[a]

[a] Dipartimento di Scienze della Terra, Università degli Studi di Roma "La Sapienza", Piazzale Aldo Moro, 5, 00185 Roma, Italy

[b] Dipartimento di Scienze dell'Ambiente e del Territorio e di Scienze della Terra, Università degli Studi di Milano-Bicocca, Piazza dell'Ateneo Nuovo, 1, 20126 Milano, Italy

Abstract

The effects of different environmental factors controlling the distribution of different morphologies, sizes and growth forms of rhodoliths in the western Pontine Archipelago have been studied. The analysis of 231 grab samples has been integrated with 68 remotely operated vehicle (ROV) videos (22 h) and a high resolution (< 1 m) side scan sonar mosaic of the seafloor surrounding the Archipelago, covering an area of approximately 460 km2. Living rhodoliths were collected in approximately 10% of the grab samples and observed in approximately 30% of the ROV dives. The combination of sediment sampling, video surveys and acoustic facies mapping suggested that the presence of rhodoliths can be associated to the dishomogeneous high backscatter sonar facies and high backscatter facies. Both pralines and unattached branches were found to be the most abundant morphological groups (50% and 41% of samples, respectively), whereas boxwork rhodoliths were less common, accounting only for less than 10% of the total number of samples. Pralines and boxwork rhodoliths were almost equally distributed among large (28%), medium (36%) and small sizes (36%). Pralines generally presented a fruticose growth form (49% of pralines) even if pralines with encrusting-warty (36% of pralines) or lumpy (15% of pralines) growth forms were also present. Morphologies, sizes and growth forms vary mainly along the depth gradient. Large rhodoliths with a boxwork morphology are abundant at depth, whereas unattached branches and, in general, rhodoliths with a high protuberance degree are abundant in shallow waters. The exposure to storm waves and bottom currents related to geostrofic circulation could explain the absence of rhodoliths off the eastern side of the three islands forming the Archipelago.

Keywords: Living rhodoliths, Mediterranean Sea, Grabs, Remotely operated vehicle, Side scan sonar

1. Introduction

Rhodoliths are formed by coralline red algae (nongeniculate Corallinales) and occur on soft substrates as free-living nodules. They represent an important, often predominant component of shelf sediments in tropical carbonate settings (Carannante et al., 1988; Canals and Ballesteros, 1997; Basso, 2012), in particular where other sources of extra-basinal silicoclastic sediment are absent, as present in the study area (Bracchi and Basso, 2012). Corallines have an important role in the carbonate budget of the present Mediterranean shallow waters which until now has been underestimated (Savini et al., 2012). Coralline red algae may support rich benthic communities (Barberá et al., 2003; Foster et al., 2013). A comparison between rhodolith beds versus sand flat communities demonstrated that the presence of rhodoliths enhances species richness and diversity in the marine benthos (Steller and Foster, 1995; Steller et al., 2003; Nelson, 2009). Rhodoliths provide three-dimensional habitats for the fauna (Hily et al., 1992; Birkett et al., 1998; Basso and Brusoni, 2004; Gherardi, 2004; Grall et al., 2006; Nelson, 2009), in particular for crustaceans, polychaetes (Harvey and Bird, 2008), cnidarians and chitons (Konar et al., 2006). Some species of the associated fauna seem to be rhodolith-specific (Steller et al., 2003), being influenced by rhodolithforming species and rhodolith morphologies (Hinojosa-Arango et al., 2004). Rhodolith beds, including maerl beds (Basso et al., 2015) are highly susceptible to ocean acidification (Martin and Gattuso, 2009; Basso, 2012) and also to the burial from fine sediments (Figueiredo et al., 2015). Fish farm waste and maerl extraction have negative effects on rhodolith and maerl communities (Wilson et al., 2004; Nelson, 2009; Aguado-Giménez and Ruiz-Fernández, 2012). Due to their ecological importance and their need to be preserved (Barberá et al., 2003; Steller et al., 2003; Hall-Spencer, 2005; Nelson, 2009), maerl beds are subject to European and UK conservation legislation (Wilson et al., 2004). In particular, L. corallioides and P. calcareum are included in annex V of the Habitats Directive. Rhodoliths and maerl preservation is particularly important also due to the slow growth rate of coralline red algae (Frantz et al., 2000; Blake and Maggs, 2003; Rivera et al., 2004; Schäfer et al., 2011), which makes them lowly resilient to environmental stress (Grall and Hall-Spencer, 2003; Wilson et al., 2004; Nelson, 2009).

The most extensive rhodolith bed has been observed off eastern Brazil, on the Abrolhos Shelf, and covers about 20,900 km2 (Amado-Filho et al., 2012). In the Mediterranean Sea, rhodolith and maerl bedshave been described on the Mallorca-Menorca shelf (Canals and Ballesteros, 1997), off the Maltese Islands (Borg et al., 1998; Sciberras et al., 2009) and in the Tyrrhenian Sea (Bressan, 1974; Basso, 1996; 1998; Di Geronimo and Giaccone, 1994; Savini et al., 2012).

In this work we report the results of the study of rhodoliths from the western Pontine Archipelago (Fig. 1a), which is located on a structural high separating Palmarola and Ventotene sedimentary

intraslope basins (Zitellini et al., 1984), in the central-eastern Tyrrhenian Sea. The Archipelago is composed of three islands (Palmarola, Ponza and Zannone), mainly formed by submarine and subaerial eruptions during the Plio-Pleistocene (Barberi et al., 1967).

The three islands are surrounded by a narrow (2–8 km wide) and steep (0.5–1.5°, up to 10° in presence of rock outcrops and canyons) continental shelf. Shelf sedimentation is mainly intrabasinal and made up of the biogenic remains of benthic communities, which act as the main sediment source for both coarse and fine sediment fractions (Bracchi and Basso, 2012). Wave metric data (http://telemisura.it) recorded for a period of 16 years (from July 1989 until June 2005) in Ponza island, show dominant wave directions from W. The area is affected by surface geostrofic marine currents flowing toward NW (Artale et al., 1994) that are deeply modified by the uneven morphology of the Archipelago and locally enhanced between islands. The tidal oscillation in the Mediterranean Sea is generally of the order of few cm, except for the north Adriatic Sea, the north Aegean Sea and the Gulf of Gabes (Tsimplis et al., 1995).

Aim of this work is to study presence, characters and distribution of living rhodoliths on the continental shelf surrounding the W Pontine Islands by integrating indirect investigation data (side-scan sonar data and remotely operated vehicle images) with a quantitative analysis of grab samples.

2. Material and methods

Grab samples, side-scan sonar (SSS) data and remotely operated vehicle (ROV) images were obtained in four oceanographic cruises carried out from 1997 to 2001 onboard the R/V Urania (CNR) and a small vessel (Vega 1) in the framework of the 1:50.000 geological mapping project funded by the Italian Geological Survey (CARG Project) (Fig. 1, Table 1).

2.1. Grab samples

Seafloor samples were collected in 2001 using a Van Veen grab (25 l). Sampling sites were targeted to groundtruth the acoustic classes depicted by side scan sonar data for the definition of both sediment texture and biological assemblages. A total of 231 stations were sampled between 10 and 250 m depth off Palmarola, Ponza and Zannone islands and La Botte Rock (Fig. 1b). For each sampling site, the slope gradient of the seafloor was measured on bathymetric data computed after actual soundings collected by the Italian Navy Hydrographical Institute (IIM).

Immediately after collection, living rhodoliths were separated from sediment and rocks, and photographed onboard to record the colour of the algal thalli for vitality estimates (Fig. 2a). According to Steneck (1986) the nodule is classified as “rhodolith” when more than 50% of the total volume of the nodule is made of coralline algae, otherwise it is classified as a “coating”. Rhodoliths were classified based on their morphology according to Basso (1998; 2012) in boxwork

(BW), pralines (PR) and unattached branches (BR) (Fig. 2b). BW are mostly irregular multispecific nodules with internal macroscopic voids filled with sediment, due to periods of growth interrupted by episodes of partial burial and/or overturning. The nucleus of a BW consists of a biogenic remains or of a small pebble. PR are mono(oligo)specific compact nodules with a biogenic or lithic nucleus, bearing variously developed protuberances at their surface. Finally, BR are monospecific rhodoliths lacking a macroscopic nucleus and possibly characterized by a high protuberance degree (Basso et al., 2009). Based on their maximum diameter, BW and PR > 1 cm in their maximum diameter were divided in large (d > 3 cm), medium (d=1.5–3 cm) and small (d <1.5 cm) rhodoliths. In addition, based on their growth form, we also divided PR in encrusting-warty, lumpy and fruticose, according to Woelkerling et al. (1993) (Fig. 2c).

Selected rhodolith samples from 15 grab stations were sectioned and observed under optical microscopy to identify species forming the algal nodule. For each sample, two perpendicular petrographic thin sections were prepared after embedding algal nodules in an epoxy resin. Mediterranean rhodoliths may show a complex composition, with occasional encrustation by bryozoans, barnacles, serpulids, and foraminifers, accompanied by a large array of dwellers (small benthic foraminifers, annelids, boring and infaunal bivalves, gastropods, chitons, articulate brachiopods, etc). The observed species diversity is associated with the 3-D structure provided by the rhodoliths (Basso et al., 2015). Macroids mainly composed by foraminifers are unknown in the Mediterranean, contrarily to tropical environments (Hottinger, 1983; Matsuda and Iryu, 2011). Since corallines are the main builders in the sedimentary environments considered here (Basso, 1998), we focussed on the identification of the most common and volumetrically important species of corallines and disregarded the thin, monostromatic thalli and the accompanying fauna. Anatomical details of corallines composing the rhodolith surface were observed in radial sections of crustose thalli, and in longitudinal sections of protuberances. Hypothallus and perithallus observations were performed at 10× magnification, whereas epithallial cells were studied at 60× magnification. The genera of the non-geniculate Corallinales were identified based on Harvey and Woelkerling (2007). Details on the anatomy and systematics of the Mediterranean corallines are reported in Basso (1995); Basso et al. (1996; 1997; Basso and Rodondi (2006) and Bressan and Babbini (2003).

2.2. ROV images

68 ROV video surveys (22 h) were conducted in June 2001 between 10 and 120 m offshore the three islands and La Botte Rock (Fig. 1). A Hyball [2] ROV equipped with a video and photo camera was used. Like grab-sampling sites, ROV sites were chosen to groundtruth the acoustic

classes defined by side scan sonar facies. ROV images were used to characterize the substrate and qualitatively estimate rhodoliths presence, abundance and habitat.

2.3. SSS data

A full-coverage, high resolution (< 1 m) side scan sonar mosaic of the seafloor surrounding the Archipelago was collected during two oceanographic cruises, in 1997 and 2001, covering an area of approximately 460 km2. A 100 kHz side scan sonar was run along contourparallel routes with 150 m per channel swath. The following six acoustic facies were identified: high backscatter (HB), rocks and high backscatter (r-HB), dishomogeneous high backscatter (D-HB), dishomogeneous low backscatter (D-LB), low backscatter (LB) and Phanerogams (i.e. Posidonia oceanica, POS) (Table 2). Sonar images were integrated with medium-resolution bathymetry derived from original soundings collected for nautical charting by the IIM (5 m isobath interval).

2.4. Statistical analysis

The univariate statistical test ANOVA was performed using the Statistica software v. 5.5, in order to establish the variation of the abundance of rhodoliths respect to depth and slope gradients, in different regions and in relation to grain size. Depth values were grouped into 5 classes (0–39 m, 40–59 m, 60–79 m, 80–110 m and > 110 m), regions into 6 groups (E islands, saddles, NE PA, NW PA, N ZA and BOTTE, Fig. 1), bottom slope into 4 groups (0–2°, > 2–3°, > 3–4° and > 4°) and grain size into 3 groups (gravel, sand and mud). Multivariate statistical analyses were also performed to test for differences among the percentage of rhodoliths with variable morphology (BW, PR and BR), size (large, medium and small) and growth form (encrusting-warty, lumpy and fruticose) versus depth, regions, slope and grain size. According to rhodoliths occurrence, 3 groups of depth were considered (40–59 m, 60–79 m and 80–110 m), as well as 4 groups of regions (saddle, NE PA, NW PA and N ZA), 4 groups of seafloor gradient (0–2°, > 2–3°, > 3–4° and > 4°) and 3 groups of grain size (gravelly sand+slightly gravelly sand (gS+(g)S), gravelly muddy sand (gmS) and muddy sandy gravel (msG)). Euclidean distances between pairs of samples were calculated to obtain a triangular distance matrix. Differences between rhodolith morphology, size and growth form at different depths, slopes and grain sizes were tested through the non-parametric analysis of similarities (ANOSIM test). ANOSIM is a resemblance-based permutation method used to test the null hypothesis of “no differences” between a priori defined groups of multivariate samples. Multivariate statistical analyses were performed with Primer software v.6 (Clarke, 1993; Clarke and Gorley, 2006).

3. Results

3.1. Grab samples

A total of 813 living rhodoliths were collected in 27 out of the 231 sampling stations. Main characters of collected samples (e.g., grain size) and sampling sites (depth, region, slope), together with rhodolith characteristics, are shown in Table 2, whereas the percentage of grabs with rhodoliths at the different depths, regions and slopes, and corresponding to the different sediment grain sizes, is shown in Fig. 3. Both PR and BR were present in 18 out of 27 grab stations (67%) and represented the most abundant morphological groups (50% and 41% of samples, respectively). BW represented the less abundant morphological group, being present in 11 out of 27 grab stations (41%), accounting only for the 9% of the total number of samples. PR and BW were almost equally distributed among large (28%), medium (36%) and small sizes (36%). PR generally presented a fruticose growth form (49% of PR) with encrusting-warty (36% of PR) or lumpy (15% of PR) growth forms subordinated. Rhodoliths were sampled in five of the six sonar facies but with an uneven distribution. In fact, HB and D-HB accounted for 65% (30% and 35%, respectively) of the specimens, whereas LB accounted for 1% (i.e. 3 specimens) (Fig. 4). The following rhodolith species were identified: Lithothamnion valens Foslie, Lithothamnion minervae Basso, Lithophyllum racemus (Lamarck) Foslie, Spongites fruticulosus Kützing and Phymatolithon calcareum (Pallas) W.H. Adey and D.L. McKibbin (Fig. 5). L. racemus was collected in 47% of grabs and represented the dominant species, followed by S. fruticulosus (40%), L. valens (33%), L. minervae (20%) and P. calcareum (7%). In some specimens, moving from the nucleus to the periphery, different species were observed.

3.2. ROV images

Living rhodoliths were observed in 21 ROV dives. In the majority of the ROV dives (43%), rhodoliths appeared associated with bifurcated and symmetrical megaripples (1–1.5 m wavelength) with low relief (usually less than 10–20 cm) (Table 3), usually hosting rhodoliths on the ripple trough. Rhodoliths were also observed in the vicinity of rocks (33% of ROV dives) and on the flat seafloor (24% of ROV dives) (Table 3). The occurrence of rhodoliths in ROV videos and side scan sonar facies indicates that they are associated to the sonar facies R-HB (48% of ROV dives), HB (29% of ROV dives), D-HB (19% of ROV dives) and LB (4% of ROV dives), thus confirming the association derived from the comparison between grab samples and sonar facies.

3.3. Statistical analysis

Results from the univariate statistical test ANOVA evidenced significant differences in the abundance of rhodoliths among the 6 sampled regions of the Archipelago (Table 4a). Based on the results of the multivariate ANOSIM test, rhodolith morphology, size and growth form were significantly different depending on depth (Table 4b).

4. Discussion

4.1. Integration of side scan sonar data, ROV dives and grab samples

In this study, we combined sediment sampling, ROV video surveys and acoustic facies mapping derived by side scan sonar data. The information provided by the three techniques is complementary. Side scan sonar data allow inferring the distribution of rhodoliths in large, deep areas. ROV video surveys are useful for groundtruthing and assessing live rhodolith distribution and habitat features. Seafloor sampling is essential to study rhodolith morphology, size, growth form and species composition. A similar approach was used in studies carried out in the south-western Atlantic Ocean and in the Mediterranean Sea in which ROV surveys suggested that specific acoustic facies can be used as a proxy of the presence of rhodoliths (Pereira-Filho et al., 2012; Savini et al., 2012). We recovered living rhodoliths mainly in the HB facies and in the D-HB facies. The HB facies relates to coarse sand and the D-HB facies relates to backscatter (usually parallel to isobaths), with prevalence of high backscatter patches. Moreover, the higher percentage of rhodoliths in the D-HB than in the D-LB facies (46% and 3%, respectively) suggests that high backscatter is enhanced by the rhodoliths themselves. These observations are consistent with other studies, such as those carried out by Micallef et al. (2012) off the Maltese archipelago and Parnum and Gavrilov (2012) in different sites around Australia, where the high backscatter intensity correlates well with rhodolith beds.

4.2. Factors controlling rhodoliths distribution in the study area

The distribution of rhodoliths is controlled by a combination of environmental variables, like temperature, salinity, irradiance, nutrients and water chemistry (Wilson et al., 2004; Teichert et al., 2012). We studied the distribution of rhodoliths with different morphology, size and growth form in the continental shelf off the western Pontine Islands. We focused on the variation of the abundance and characteristics of rhodoliths along water depth and slope gradients, and in different regions, whose combinations are proxies of different oceanographic settings.

4.2.1. Water depth

The relationship between rhodoliths and water depth depends on the variation along the depth gradient of environmental variables affecting algae, like light availability and hydrodynamic regime at the seafloor. In addition, the input of terrigenous material from subaerialcoastal erosion, and therefore rhodoliths exposure to sediment burial, is higher at shallow water than at depth. Finally, species zonation and the transport of rhodoliths from the continental shelf to deeper waters vary with depth and may also control rhodoliths distribution. The bathymetric distribution of the sampling stations in the study area is rather homogeneous, with a higher concentration between 60 and 110 m w.d. (Fig. 3a). The deepest rhodolith findings (112 m depth at station PO-ZA 5) match

the lowest bathymetric limit of the photic zone in the western Mediterranean Sea (Di Geronimo and Giaccone, 1994; Basso, 1996). In our study, the high tolerance of rhodoliths to different intensities of light is confirmed by the wide bathymetrical distribution of rhodolith-associated megaripples (from 45 to 114 m depth) and of rhodolith-associated sonar facies (from 20 to 100 m depth). According to Basso (1996), among macrobenthic algae, the non-geniculate corallines show the widest depth range. Depending on the species, the upper limit of their depth range can be related to the risk of desiccation or can depend on photosynthesis inhibition under high-irradiance conditions (Basso, 1996; Wilson et al., 2004; Basso et al., 2009). As regards the deepest limit of their distribution, red algae are well adapted to live in dim light conditions (Kühl et al., 2001), both in deep waters (Littler et al., 1985; Lavrado, 2006; Figueiredo et al., 2012) and in polar regions (Freiwald and Henrich, 1994; Wiencke and Clayton, 2002; Roberts et al., 2002; Teichert et al., 2012). In our study, water depth seems to be the best proxy for rhodoliths morphology, size and growth form (Table 4b). The reverse distribution of BW and BR, with the first increasing with depth and the latter decreasing (Fig. 6a), is in agreement with the high protuberance degree that characterizes rhodoliths living under high energy conditions, like the maerl species Phymatholithon calcareum and Lithothamnion corallioides, which is related to the apical abrasion resulting from frequent overturning (Bosence and Pedley, 1982; Basso, 1996). On the contrary, in deeper settings, the fine sediment which accumulates among the concentric algal strata prevents the formation of compact nodules, fostering the growth of BW. The low hydrodynamics typical of deep seafloor is responsible for the asymmetric growth-form characterizing the BW morphological group (Basso, 1998). In the study area, BW showed a bimodal distribution with depth (Fig. 6a); we suggest that the deepest samples may represent recent colonizations of relict BW. The presence of larger rhodoliths in deeper water (Fig. 6b) is in agreement with previous studies carried out in the southern coast of Espírito Santo State (Brazil) (Amado-Filho et al., 2007) and off Newfoundland and Labrador (Canada) (Gagnon et al., 2012), but contrasts with the lack of relationship between depth and nodules diameter found by Peña and Bárbara (2008) or with the inverse relationship found by other authors (Littler et al., 1991; Steller and Foster, 1995; Riul et al., 2009; Bahia et al., 2010). The direct relationship between size and water depth suggests that size increases at high depths thanks to the infrequent motion of rhodoliths, which is related to the reduced bottom currents and the limited bioturbation (Marrack, 1999) and competition with soft-bodied algae. A bias may exist between rhodolith morphologies (Fig. 6a) and size (Fig. 6b), as BW are always larger than PR and BR. PR and BR would need high hydrodynamic energy to become large rhodoliths while maintaining their morphology. Probably, PR and BR, at some time of their growth, die buried or stop moving and transform into BW. Finally, the variation in the protuberance degree may be speciesspecific (Steller

and Foster, 1995), but a reduced rhodolith motion at depth could also be responsible for the low protuberance degree characterising deep rhodoliths in the study area (Fig. 6c), as it has been observed in other studies (Foster et al., 1997).

4.2.2. Region

The distribution of the sampling stations in the study area is rather homogeneous (Fig. 3b) and our results suggest that exposure to storm waves (i.e., bottom currents related to wave action), along with bottom currents due to local forcing of geostrophic circulation, should represent the main factors controlling the occurrence of rhodoliths at comparable depths (Table 4a). Moderate hydrodynamics are considered adequate for rhodoliths (Ryan et al., 2007) and preferable than lowest and highest energies. Low hydrodynamics seem to prevent rhodolith formation by smothering from excessive fine sedimentation and, in agreement with the wave data collected at the meteorological station located in Ponza, could explain the absence of rhodoliths off the eastern side of the three islands forming the Archipelago (Fig. 3b). High hydrodynamics are useful to prevent fouling (Steller and Foster, 1995) and the burial of the algal nodules, but can cause rhodoliths excessive abrasion or their transport out of favourable growing conditions (Marrack, 1999; Foster, 2001). However, in our study, we found that the action of relatively strong bottom currents suggested by the presence of bedforms and particular SSS facies (dishomogenous high backscatter related to coarse-grained sediment belts) did not prevent the presence of rhodoliths. Overturning influences the morphology of rhodoliths, and, for this reason, the distribution of different morphologies is related to bottom currents (Post et al., 2006; Basso et al., 2009). In the study area, the high percentage of BW and of rhodoliths with an encrusting-warty growth form off NE Palmarola (Fig. 7a and c) is in accordance with the presence of westerly storm waves (Fig. 1). Additionally, the high percentage of PR both along the saddle between Palmarola and Ponza and the saddle between Ponza and Zannone (Fig. 7a) agrees with relatively strong bottom currents hypothesized for the saddles between the islands. It also confirms the results of tank experiments and field observations, showing a correlation between high protuberance degree of fruticose rhodoliths and exposure to currents (Bosence, 1976; Basso and Tomaselli, 1994). Nevertheless, we did not find statistically significant correlations between the factor “region” and the morphology, size or growth form of rhodoliths (Table 4b).

4.2.3. Seafloor slope gradient

The seafloor slope gradient measured on medium-resolution bathymetric data indicates the “overall” slope of the seafloor and does not reflect microtopography, that in some ROV images appears to be relevant for rhodoliths occurrence. Slope varies between 0 and 10° and the distribution of sampling stations is rather homogeneous (Fig. 3c). We did not find a statistically

significant correlation between bottom slope and the percentage of grabs with rhodoliths (Table 4a). Rhodoliths were always absent from areas with slope values higher than 6° (Fig. 3c), but we also observed an unexpected high percentage of large BW and rhodoliths with an encrusting-warty growth form in relatively steep bottoms (slope > 3°) (Fig. 8).

4.2.4. Sediment grain size

In the western Pontine Archipelago, samples had different percentages of mud (d < 0.063 mm), sand (0.063 mm< d < 2 mm) and gravel (d > 2 mm). According to Folk (1954) grain size classification, in our study, rhodoliths appeared associated to muddy sandy gravel (msG) (33% of grabs with rhodoliths), gravelly sand (gS) (27%), slightly gravelly sand ((g)S) (14%) and gravelly muddy sand (gmS) (13%) (Fig. 3d). Even if the data indicate a direct relationship between coarse sediment and presence of rhodoliths (Fig. 9), the amount of muddy sediment varied considerably among stations with rhodoliths (it varied between ~2% at station PO-PA 13 and ~43% at station PO-ZA 5). This would indicate that locally rhodoliths may develop also under low hydrodynamic conditions. Although we did not find a significant correlation between sediment grain size and the presence (Table 4a) or the characteristics (Table 4b) of living rhodoliths, they appeared preferably associated with sandy sediment with gravel of bioclastic origin, therefore, to the biocenosis of the coastal detritic bottom (Pérès and Picard, 1964).

4.3. Rhodolith-forming species

In our samples, Phymatolithon calcareum was identified only in one station (NW PA2), where it was present as BR (Table 1). This fact is in agreement with the idea that this species, together with Lithothamnion corallioides, have a species-specific fruticose growthform (Basso, 1994). The occurrence of L. valens, that more rarely corresponds to the BR morphology (Basso, 1995), corresponded to the presence of BR at stations PO-PA6, PO-PA13 and N ZA1, but not at stations PO-PA11 and PO-PA14, where it formed PR and BW (Table 1). PR were found at the three stations were Lithothamnion minervae (Basso, 1998) was identified. On the contrary, PR were found only at five of the seven stations where Lithophyllum racemus, another species related to the formation of PR (Basso, 1996), was identified (Table 1). Our results confirm that rhodolith morphology can be related to the algal species forming the nodule surface (Basso, 1996), as expected from the correlation between morphology and depth gradient. It is also clear that the overall morphological variation within rhodolith species is large (Riosmena-Rodriguez et al., 1999).

5. Conclusions

As a whole, The seafloor classification based on acoustic backscatter performed at western Pontine Archipelago provides a tool to adequately map benthic habitats. The combination of sediment

sampling, ROV video surveys and acoustic facies derived by side scan sonar data confirmed that the presence of rhodoliths can be associated to specific acoustic facies. In particular, rhodoliths are mainly associated with the dishomogeneous high backscatter sonar facies and the high backscatter facies, which are related to sandy sediment with gravel of bioclastic origin, although no significant correlation was found between sediment grain size and the occurrence or the characteristics of living rhodoliths. In addition, based on ROV data, rhodoliths appear associated with megaripples, thus confirming as favouring factor an active hydrodynamics affecting the seafloor, even if not particularly high-energy as half of the specimen with rhodoliths contains more than 30% of mud. Both pralines and unattached branches were found to be the most abundant morphological groups, whereas boxwork rhodoliths are less common, accounting only for less than 10% of the total number of samples. Pralines and boxwork rhodoliths were almost equally distributed among large, medium and small sizes, although boxwork rhodoliths reach the largest size. Pralines generally presented a fruticose growth form even within a large variability, since encrusting- warty or lumpy growth forms were also present. After considering the effects of water depth, region, seafloor slope gradient and grain size on the distribution of rhodoliths with different abundance, morphology, size and growth form, the main factor controlling rhodolith morphology is the depth gradient, with unattached branches decreasing with depth and boxwork rhodoliths increasing. At comparable depths, the exposure to storm waves along with bottom currents due to morphological forcing of geostrophic circulation represents the main factor controlling the abundance of rhodoliths and could explain their absence off the eastern side of the three islands forming the Archipelago. Finally, our results confirm that rhodolith morphology is related to the algal species forming the nodule surface, as shown by the praline-forming *L. minervae* and *L. racemus*.

References

Aguado-Giménez, Ruiz-Fernández, 2012. Influence of an experimental fish farm on the spatio-temporal dynamic of a Mediterranean maërl algae community. Mar. Environ. Res. 74, 47-55.

Amado-Filho, G.M., Maneveldt, G., Manso, R.C.C., Marins-Rosa, B.V., Pacheco, M.R., Guimarães, S.M.P.B., 2007. Structure of rhodolith beds from 4 to 55 m deep along the southern coast of Espírito Santo State, Brazil. Cienc. Mar. 33, 399-410. Amado-Filho, G.M., Moura, R.L., Bastos, A.C., Salgado, L.T., Sumida, P.Y., Guth, A.Z., Francini-Filho, R.B., Pereira-Filho, G.H., Abrantes, D.P., Brasileiro, P.S., Bahia, R.G., Leal, R.N., Kaufman, L., Kleypas, J.A., Farina, M., Thompson, F.L., 2012. Rhodolith Beds Are Major $CaCO_3$ Bio-Factories in the Tropical South West Atlantic. PLoS ONE. ⟨http://dx.doi.org/10.1371/journal.pone.0035171⟩.

Artale, V., Astraldi, M., Buffoni, G., Gasparini, G.P., 1994. Seasonal variability of gyrescale circulation in the northern Tyrrhenian Sea. J. Geophys. Res. - Oceans 99 (C7), 14127-14137.

Bahia, R.G., Abrantes, D.P., Brasileiro, P.S., Pereira Filho, G.H., Amdo Filho, G.M., 2010. Rhodolith bed structure along a depth gradient on the northern coast of Bahia State, Brazil. Braz. J. Oceanogr. 58, 323-337.

Barberá, C., Bordehore, C., Borg, J.A., Glemarec, M., Grall, J., Hall-Spencer, J.M., De La Huz, C., Lanfranco, E., Lastra, M., Moore, P.G., Mora, J., Pita, M.E., Ramos-Espla, A.A., Rizzo, M., Sanchez-Mata, A., Seva, A., Schembri, P.J., Valle, C., 2003. Conservation and management of Northeast Atlantic and Mediterranean maërl beds. Aquat. Conserv.: Mar. Freshw. Ecosyst. 13, S65-S76.

Barberi, F., Borsi, S., Ferrara, G., Innocenti, F., 1967. Contributo alla conoscenza vulcanologica e magmatologica delle isole dell' Arcipelago Pontino. Mem. Soc. Geol. Ital. 6, 581-606.

Basso, D., 1994. Study of living calcareous algae by a paleontological approach: the nongeniculate Corallinaceae (Rhodophyta) of the soft bottoms of the Tyrrhenian Sea (Western Mediterranean). The genera Phymatolithon Foslie and Mesophyllum Lemoine. Riv. Ital. Paleontol. Stratigr. 100, 575-596.

Basso, D., 1995. Living calcareous algae by a paleontological approach: the genus Lithothamnion Heydrich nom. cons. from the soft bottoms of the Tyrrhenian Sea (Mediterranean). Riv. Ital. Paleontol. Stratigr. 101, 349-366.

Basso, D., 1996. Adaptative strategies and convergent morphologies in some Mediterranean coralline algae, in Cerchi, A., ed., Autoecology of Selected Fossil Organisms: Achievements and Problems: Boll. Soc. Paleont. Ital. 3, pp. 1-8.

Basso, D., 1998. Deep rhodolith distribution in the Pontian Islands, Italy: a model for the paleoecology of a temperate sea. Palaeogeogr. Palaeocl. 137, 173-187.

Basso, D., 2012. Carbonate production by calcareous red algae and global change. Geodiversitas 34, 13-33.

Basso, D., Tomaselli, V., 1994. Paleoecological potentiality of rhodoliths: a Mediterranean case history. In: Matteucci, R., Carboni, M.G., Pignatti, J.S. (Eds.). Studies on Ecology and Paleoecology of Benthic Communities. Boll. Soc. Paleontol. Ital. Spec. Vol. 2, pp. 17-27.

Basso, D., Brusoni, F., 2004. The molluscan assemblage of a transitional environment: the Mediterranean maerl from off the Elba Island (Tuscan Arcipelago, Tyrrhenian Sea). Boll. Malacol. 40, 37-45.

Basso, D., Rodondi, G., 2006. A Mediterranean population of Spongites fruticulosus (Rhodophyta, Corallinales), the type species of Spongites, and the taxonomic status of S. stalactitica and S. racemosa. Phycologia 45, 403-416.

Basso, D., Fravega, P., Vannucci, G., 1996. Fossil and living corallinaceans related to the Mediterranean endemic species Lithophyllum racemus (Lamarck) Foslie. Facies 35, 275-292.

Basso, D., Fravega, P., Vannucci, G., 1997. The taxonomy of Lithothamnion ramosissimum (Gümbel non Reuss) Conti and Lithothamnion operculatum (Conti) Conti (Rhodophyta, Corallinaceae). Facies 37, 167-182.

Basso, D., Rodondi, G., Mari, M., 2004. A comparative study between Lithothamnion minervae and the type material of Millepora fasciculata (Corallinales, Rhodophyta). Phycologia 43, 215-223.

Basso, D., Nalin, R., Nelson, C.S., 2009. Shallow-water Sporolithon rhodoliths from North Island (New Zealand). Palaios 24, 92-103.

Basso, D., Babbini, L., Kaleb, S., Bracchi, V.A., Falace, A., 2015. Monitoring deep Mediterranean rhodolith beds. Aquatic Conserv: Mar. Freshw. Ecosyst. (2015). Published online in Wiley Online Library (wileyonlinelibrary.com). ⟨http://dx.doi. org/10.1002/aqc.2586⟩.

Birkett, D.A., Maggs, C., Dring, M.J., 1998. Maerl: an overview of dynamic and sensitivity characteristics for conservation management of marine SACs. Scott. Assoc. Mar. Sci. 5, 1-90.

Blake, C., Maggs, C.A., 2003. Comparative growth rates and internal banding periodicity of maërl species (Corallinales, Rhodophyta) from northern Europe. J. Phycol. 42, 606-612.

Borg, J.A., Howege, H.M., Lanfranco, E., Micallef, S.A., Mifsud, C., Schrembri, P.J., 1998. The macrobenthic species of the infralittoral to circalittoral transition zone off the northeastern coast of Malta (central Mediterranean). Xjenza 3, 16-24.

Bosence, D.W.J., 1976. Ecological studies on two unattached coralline algae from western Ireland. Palaeontology 19, 365-395.

Bosence, D.W.J., Pedley, H.M., 1982. Sedimentology and Paleoecology of a Miocene coralline algal biostrome from the Maltese Islands. Palaeogeogr. Palaeoclimatol. Palaeoecol. 38, 9-43.

Bracchi, V.A., Basso, D., 2012. The contribution of calcareous algae to the biogenic carbonates of the continental shelf: Pontian Islands, Tyrrhenian Sea, Italy, in Basso D. & Granier B. (eds), Calcareous algae and global change: from identification to quantification. Geodiversitas 34, pp. 61-76.

Bressan, G., 1974. Rodoficee calcaree dei mari italiani. Boll. Soc. Adriat. Sc. Nat. Trieste 59, 1-132.

Bressan, G., Babbini, L., 2003. Corallinales del Mediterraneo: guida alla determinazione. Biol. Mar. Mediterr. 10 (Suppl. 2), 237.

Canals, M., Ballesteros, E., 1997. Production of carbonate particles by phytobenthic communities on the Mallorca-Menorca shelf, northwestern Mediterranean Sea. Deep-Sea Res II 44, 611-629.

Carannante, G., Esteban, M., Milliman, J.D., Simone, L., 1988. Carbonate lithofacies as paleolatitude indicators: problems and limitations. Sediment. Geol. 60, 333-346.

Clarke, K.R., 1993. Non-parametric multivariate analyses of changes in community structure. Australian. J. Ecol. 18, 117-143.

Clarke, K.R., Gorley, R.N., 2006. PRIMER v6: User Manual/tutorial. PRIMER-E, Plymouth UK.

Di Geronimo, R., Giaccone, G., 1994. Le alghe calcaree del Detritico Costiero di Lampedusa (Isole Pelagie): boll. Acc. Gioenia Sci. Nat. Catania 27, 75-96.

Figueiredo, M.A.O., Coutinho, R., Villas-Boas, A.B., Tâmega, F.T.S., Mariath, R., 2012. Deep water rhodolith productivity and growth in the southwestern Atlantic. J. Appl. Phycol. 24, 487-493.

Figueiredo, M.A.O., Eide, I., Reynier, M., Villas-Bôas, A.B., Tâmega, F.T.S., Ferreira, C.G., Nilssen, I., Coutinho, R., Johnsen, S., 2015. The effect of sediment mimicking drill cuttings on deep water rhodoliths in a flow-through system: experimental work and modeling. Mar. Pollut. Bull. 95, 81-88.

Folk, R.L., 1954. The distinction between grain size and mineral composition in sedimentary rock nomenclature. J. Geol. 62 (4), 344-359.

Foster, M.S., 2001. Rhodoliths: between rocks and soft places. J. Phycol. 37, 659-667. Foster, M.S., Riosmena-Rodríguez, R., Steller, D.L., Woelkerling, W.J., 1997. Living rhodolith beds in the Gulf of California and their implications for paleoenvironmental interpretation. Geol. Soc. Am. Bull. 318, 127-139.

Foster, M.S., Amado-Filho, G.M., Kamenos, N.A., Riosmena-Rodriguez, R., Steller, D.L., 2013. Rhodoliths and rhodolith beds. Smithson. Contrib. Mar. Sci. 39, 143-155.

Frantz, B.R., Kashgarian, M., Coale, K.H., Foster, M.S., 2000. Growth rate and potential climate record from a rhodolith using ^{14}C accelerator mass spectrometry. Limnol. Oceanogr. 45, 1773-1777.

Freiwald, A., Henrich, R., 1994. Reefal coralline algal build-ups within the Arctic Circle: morphology and sedimentary dynamics under extreme environmental seasonality. Sedimentology 41, 963-984.

Gagnon, P., Matheson, K., Stapleton, M., 2012. Variation in rhodolith morphology and biogenic potential of newly discovered rhodolith beds in Newfoundland and Labrador (Canada). Bot. Mar. 55, 85-99.

Gherardi, D.F.M., 2004. Community structure and carbonate production of a temperate rhodolith bank from Arvoredo Island, Southern Brazil. Braz. J. Oceanogr. 52, 207-224.

Grall, J., Hall-Spencer, J.M., 2003. Problems facing maërl conservation in Brittany. Aquat. Conserv. Mar. Freshw. Ecosyst. 13, 55-64.

Grall, J., Le Loch, F., Guyonnet, B., Riera, P., 2006. Community structure and food web based on stable isotopes (δ15N and δ13C) analyses of a North Eastern Atlantic maerl bed. J. Exp. Mar. Biol. Ecol. 338, 1-15.

Hall-Spencer, J., 2005. Ban on maërl extraction. Mar. Poll. Bull. 50, 121.

Harvey, A.S., Woelkerling, W.J., 2007. A guide to nongeniculate coralline red algal (Corallinales, Rhodophyta) rhodolith indentification. Cienc. Mar. 33, 411-426.

Harvey, A.S., Bird, F.L., 2008. Community structure of a rhodolith bed from coldtemperate waters (southern Australia). Aust. J. Bot. 56, 437-450.

Hily, C., Potin, P., Floch, J.Y., 1992. Structure of subtidal algal assemblages on soft bottom sediments: fauna/flora interactions and role of disturbances in the Bay of Brest, France. Mar. Ecol. Prog. Ser. 85, 115-130.

Hinojosa-Arango, G., Riosmena-Rodriguez, R., 2004. Influence of rhodolith-forming species and growth-form on associated fauna of rhodolith beds in the central-west Gulf of California, México. Mar. Ecol. 25, 109-127.

Hottinger, L., 1983. Neritic macroid genesis, an ecological approach. In: Peryt, T.M. (Ed.), Coated Grains. Springer-Verlag, Berlin Heidelberg, 38-55.

Konar, B., Riomena-Rodriguez, R., Iken, K., 2006. Rhodolith bed: a newly discovered habitat in the North Pacific Ocean. Bot. Mar. 49, 355-359.

Kühl, M., Glud, R.N., Borum, J., Roberts, R., Rysgaard, S., 2001. Photosynthetic performance of surface-associated algae below sea ice as measured with a pulseamplitude- modulated (PAM) fluorometer and O_2 microsensors. Mar. Ecol. -Prog. Ser. 223, 1-14.

Lavrado, H.P., 2006. Caracterização do ambiente e da comunidade bentônica. In: Lavrado, H.P., Ignácio, B.L. (Eds.), In Biodiversidade da Costa Central Da Zona Econômica Exclusiva Brasileira. Museu Nacional, Rio de Janeiro, 19-66.

Littler, M.M., Littler, D.S., Blair, S.M., Norris, J.N., 1985. Deepest known plant life discovered on an uncharted seamount. Science 227, 57-59.
Littler, M.M., Littler, D.S., Hanisak, M.D., 1991. Deep-water rhodolith distribution, productivity, and growth history at sites of formation and subsequent degradation. J. Exp. Mar. Biol. Ecol. 150, 163-182.
Marrack, E.C., 1999. The relationship between water motion and living rhodolith beds in the southwestern Gulf of California, Mexico. Palaios 14, 159-171.
Martin, S., Gattuso, J.-P., 2009. Response of Mediterranean coralline algae to ocean acidification and elevated temperature. Glob. Chang. Biol. 15 (8), 2089-2100.
Matsuda, S., Iryu, Y., 2011. Rhodoliths from deep fore-reef to shelf areas around Okinawa-jima, Ryukyu Islands, Japan. Mar. Geol. 282, 215-230.
Micallef, A., Le Bas, T.P., Huvenne, V.A.I., Blondel, pH, Hühnerbach, V., Deidun, A., 2012. A multi-method approach for benthic habitat mapping of shallow coastal areas with high-resolution multibeam data. Cont. Shelf Res 39-40, 14-26.
Nelson, W.A., 2009. Calcified macroalgae critical to coastal ecosystems and vulnerable to change: a review. Mar. Freshw. Res. 60, 787-801.
Parnum, I., Gavrilov, A. 2012. High-frequency seafloor acoustic backscatter from coastal marine habitats of Australia. Proceedings of Acoustics, 21-23 November 2012, Fremantle, Australia.
Peña, V., Bárbara, I., 2008. Biological importance of an Atlantic European maërl bed off Benencia Island (northwest Iberian Peninsula). Bot. Mar. 51, 493-505.
Pereira-Filho, G.H., Amado-Filho, G.M., de Moura, R.L., Bastos, A.C., Guimarães, S.M.P.B., Salgado, L.T., Francini-Filho, R.B., Bahia, R.G., Pinto Abrantes, D., Guth, A.Z., Brasileiro, P.S., 2012. Extensive rhodolith beds cover the summits of Southwestern Atlantic Ocean Seamounts. J. Coast. Res. 28, 261-269.
Pérès, J.M., Picard, J., 1964. Nouveau manuel de binomie benthique de la Méditerranée. Rec. Trav. Stat. Mar. Endoume 31, 1-37.
Post, A.L., Wassenberg, T.J., Passlow, V., 2006. Physical surrogates for macrofaunal distributions and abundance in a tropical gulf. Mar. Freshw. Res. 57, 469-483.
Riosmena-Rodríguez, R., Woekerling, Wm.J., Foster, M.S., 1999. Taxonomic reassessment of rhodolith-forming species of Lithophyllum (Corallinales, Rhodophyta) in the Gulf of California, Mexico. Phycologia 38, 401-417.
Riul, P., Lacouth, P., Roberto Pagliosa, P., Lindsey Christoffersen, M., Antunes Horta, P., 2009. Rhodolith beds at the easternmost extreme of South America: community structure of an endangered environment. Aquat. Bot. 90, 315-320.
Rivera, M.G., Riosmena-Rodriguez, R., Foster, M.S., 2004. Age and growth of Lithothamnion muelleri (Corallinales, Rhodophyta) in the southwestern Gulf of California, Mexico. Cienc. Mar. 30, 235-249.
Roberts, R.D., Kühl, M., Glud, R.N., Rysgaard, S., 2002. Primary production of crustose coralline red algae in a high Arctic fjord. J. Phycol. 38, 273-283.
Ryan, D.A., Brooke, B.P., Collins, L.B., Kendrick, G.A., Baxter, K.J., Bickers, A.N., Siwabessy, P.J.W., Pattiaratchi, C.B., 2007. The influence of geomorphology and sedimentary processes on shallow-water benthic habitat distribution: esperance Bay, Western Australia. Estuar. Coast. Shelf Sci. 72, 379-386.
Savini, A., Basso, D., Bracchi, V.A., Corselli, C., Pennetta, M., 2012. Maerl-bed mapping and carbonate quantification on submerged terraces offshore the Cilento peninsula (Tyrrhenian Sea, Italy), in Basso D. & Granier B. (eds), Calcareous algae and global change: from identification to quantification. Geodiversitas 34, pp. 77-98.
Sciberras, M., Rizzo, M., Mifsud, J.R., Camilleri, K., Borg, J.A., Lanfranco, E., Schembri, P.J., 2009. Habitat structure and biological characteristics of a maerl bed off the northeastern coast of the Maltese Islands (centeral Mediterranean). Mar. Biodivers. 39, 251-264.
Schäfer, P., Fortunato, H., Bader, B., Liebetrau, V., Bauch, T., Reijmer, J.J.G., 2011. Growth rates and carbonate production by coralline red algae in upwelling and nonupwelling settings along the Pacific coast of Panama. Palaios 26, 420-432.
Steller, D.L., Foster, M.S., 1995. Environmental factors influencing distribution and morphology of rhodoliths in Bahía Concepción, B.C.S., Mexico. J. Exp. Mar. Biol. Ecol. 194, 201-212.
Steller, D.L., Riosmena-Rodriguez, R., Foster, M.S., Roberts, C., 2003. Rhodolith bed diversity in the Gulf of California: the importance of rhodolith structure and consequences of anthropogenic disturbances. Aquat. Conserv. Mar. Freshw. Ecosyst. 13, S5-S20.
Steneck, R.S., 1986. The ecology of coralline algal crusts: convergent patterns and adaptative strategies. Annu. Rev. Ecol. Syst. 17, 273-303.
Teichert, S., Woelkerling, W., Rüggeberg, A., Wisshak, M., Piepenburg, D., Meyerhöfer, M., Form, A., Büdenbender, J., Freiwald, A., 2012. Rhodolith beds (Corallinales, Rhodophyta) and their physical and biological environment at 80°31′ N in Nordkappbukta (Nordaustlandet, Svalbard Archipelago, Norway). Phycologia 51, 371-390.
Tsimplis, M.N., Proctor, R., Flather, R.A., 1995. A two-dimensional tidal model for the Mediterranean Sea. J. Geophys. Res. 100. http://dx.doi.org/10.1029/95JC01671, (issn: 0148-0227).
Wilson, S., Blake, C., Berges, J.A., Maggs, C.A., 2004. Environmental tolerances of freeliving coralline algae (maerl): implications for European marine conservation. Biol. Conserv. 120, 279-289.
Wiencke, C., Clayton, M.N., 2002. Antarctic Seaweeds. A.R.G. Gantner Verlag, Ruggell, Lichtenstein, 239.
Woelkerling, W.J., Irvine, L.M., Harvey, A.S., 1993. Growth-forms in non-geniculate coralline red algae (Corallinales, Rhodophyta). Aust. Syst. Bot. 6, 277-293. Zitellini, N., Marani, M., Borsetti, A., 1984. Post-orogenic tectonic evolution of Palmarola and Ventotene basins (Pontine Archipelago). Mem. Soc. Geol. Ital. 27, 121-131.

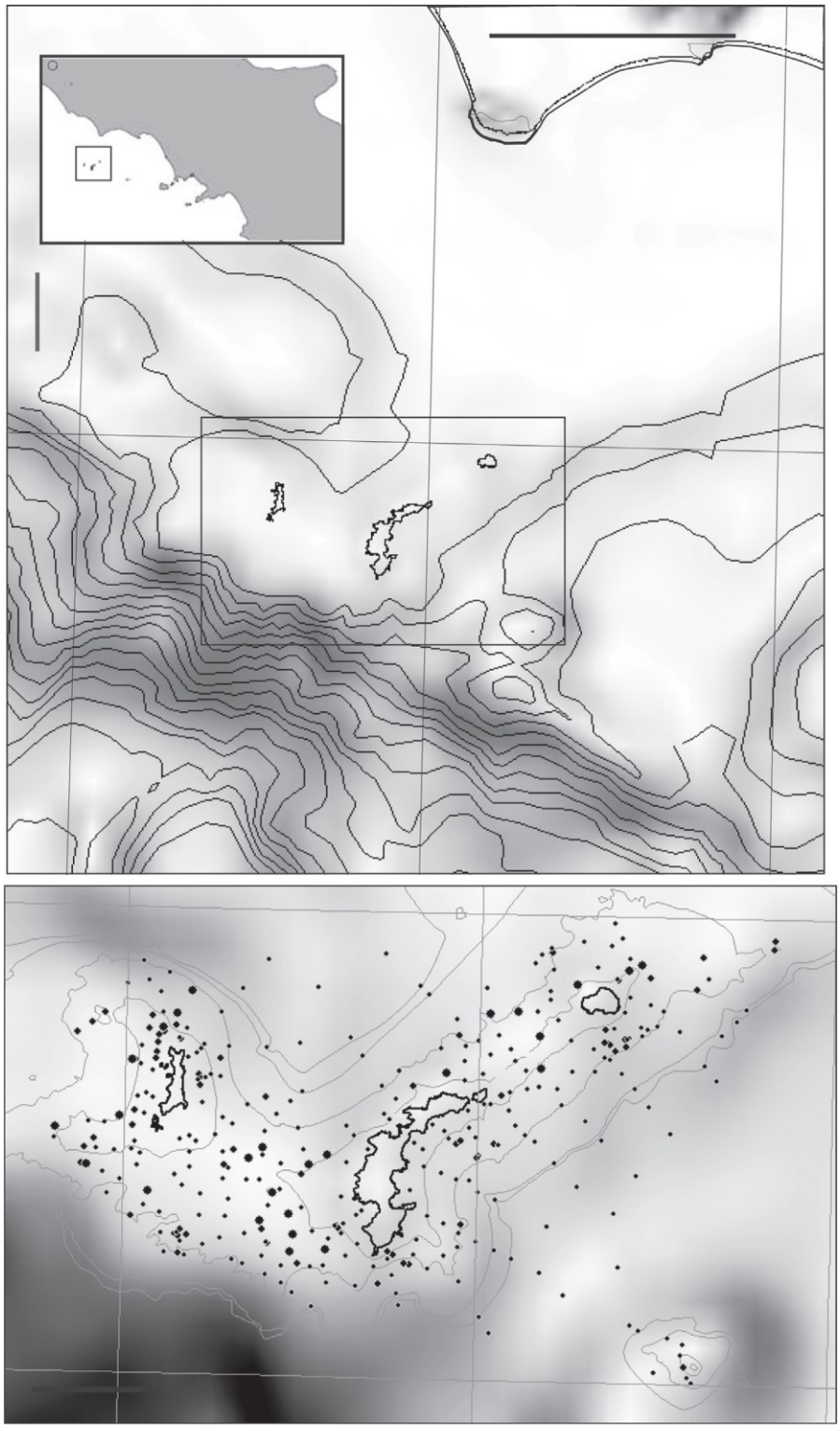

Fig. 1. Study area with sampling stations in Ponza.

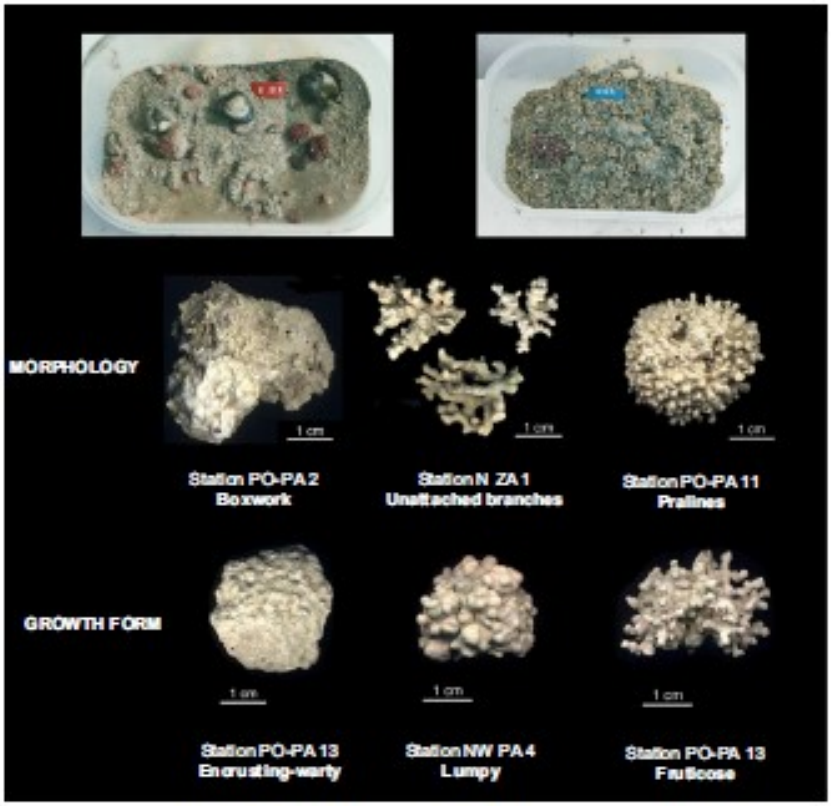

Fig. 2. Living rhodoliths photographed onboard (a), rhodolith morphology (b) and growth form (c).

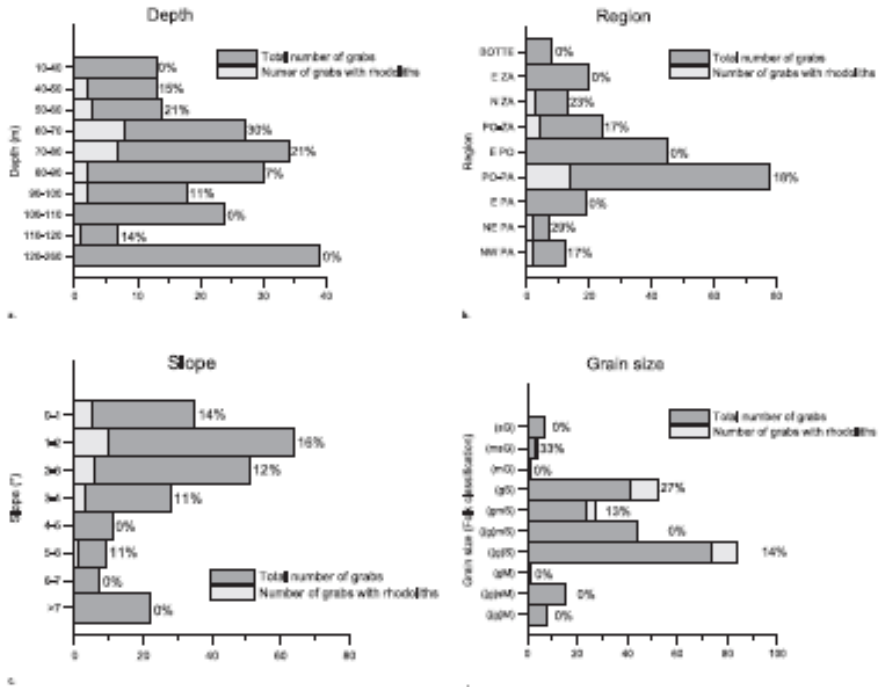

Fig. 3. (a) Relative and absolute abundance of grabs with rhodoliths with respect to the total number of grabs at different water depths. Total number of grabs in each depth interval: 13 (10–40 m); 13 (40–50 m); 14 (50–60 m); 27 (60–70 m); 34 (70–80 m); 30 (80–90 m); 18 (90–100 m); 24 (100–110 m); 7 (110–120 m); 39 (120–260 m). (b) Relative and absolute abundance of grabs with rhodoliths with respect to the total number of grabs at the different regions. Note how the eastern sectors of the islands (*) lack rhodoliths. Number of grabs in each region: 12 (NW PA); 7 (NE PA); 19 (E PA); 78 (PO-PA); 45 (E PO); 24 (PO-ZA); 13 (N ZA); 20 (E ZA); 8 (BOTTE). (c) Relative and absolute abundance of grabs with rhodoliths with respect to the total number of grabs at different slopes. Number of grabs in each slope interval: 35 (0–1°); 64 (> 1–2°); 51 (> 2–3°); 28 (> 3–4°); 11 (> 4–5°); 9 (> 5–6°); 7 (> 6–7°); 22 (> 7°). (d) Relative and absolute abundance of grabs with rhodoliths with respect to the total number of grabs corresponding at different sediment grain size. Number of grabs corresponding to each sediment grains size group: 8 ((g)M); 15 ((g)sM); 1 (gM); 74 ((g)S); 44 ((g)mS); 24 (gmS); 41 (gS); 1 (mG); 3 (msG); 7 (sG).

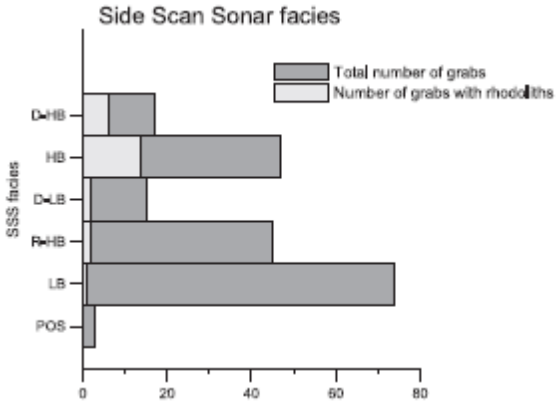

Fig. 4. Percentage of grabs with rhodoliths with respect to the total number of grabs corresponding to each side scan sonar facies. (D-HB: dishomogeneous high backscatter; HB: high backscatter; D-LB: dishomogeneous low backscatter; R-HB: rocks high backscatter; LB: low backscatter; POS: marine fanerogame, i.e. Posidonia oceanica). (Number of grabs in each acoustic facies: D-HB: 17; HB: 47; D-LB: 15; R-HB: 45; LB: 74; POS: 3).

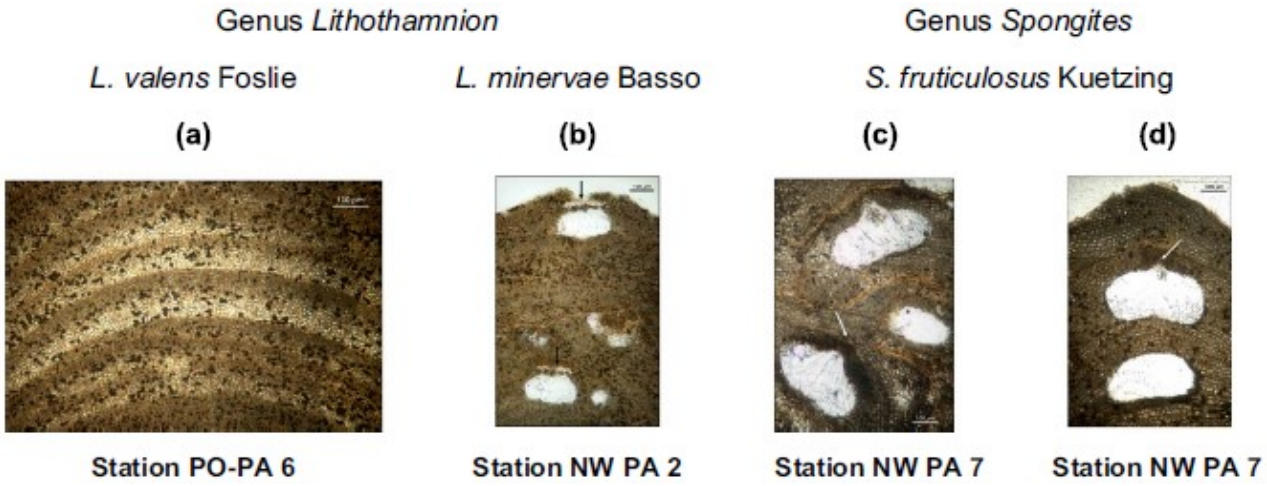

Fig. 5. Anatomical feature of dominant coralline algae.

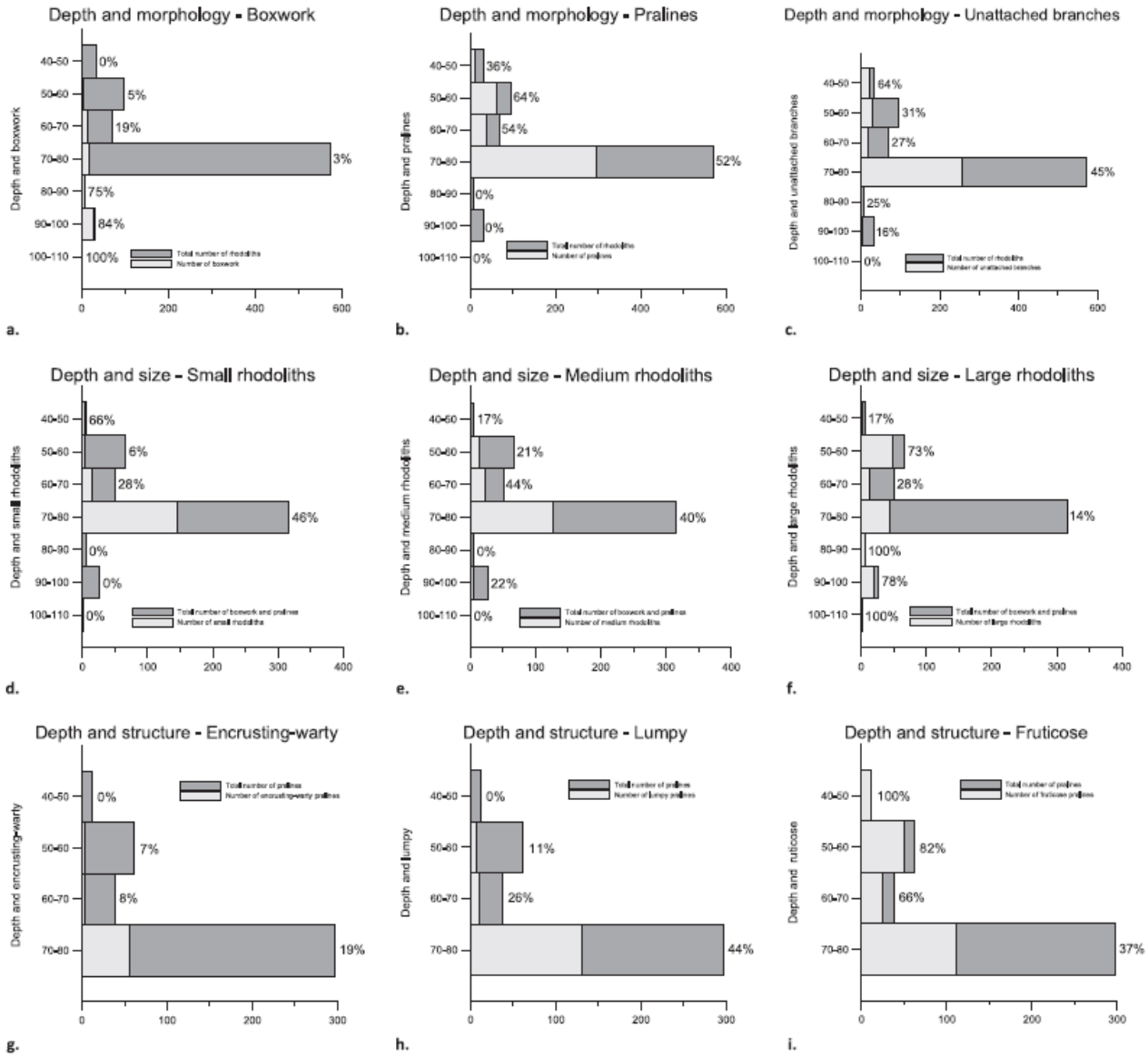

Fig. 6. Effects of depth on rhodolith morphology, size and growth form. Relative and absolute abundance of BW (a), PR (b) and BR (c) with respect to the total number of rhodoliths at different water depths. Relative and absolute abundance of small (d), medium (e) and large (f) rhodoliths with respect to the sum of BM and PR at different water depths. Relative and absolute abundance of PR with encrusting-warty (g), lumpy (h) and fruticose (i) growth form with respect to the total number of PR at different water depths.

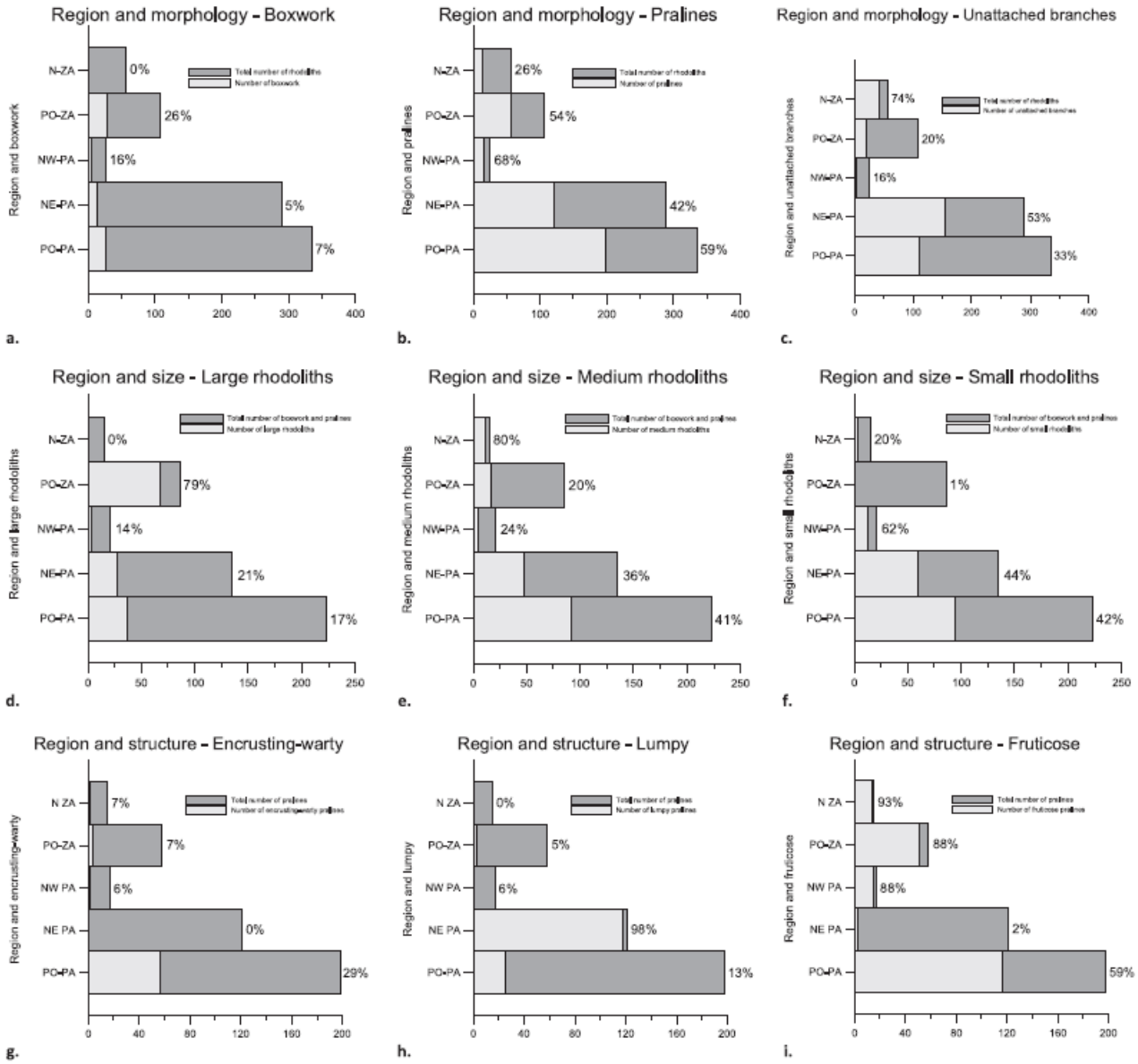

Fig. 7. Effects of the region on rhodolith morphology, sizes and growth form. Percentage of BW (a), PR (b) and BR (c) with respect to the total number of rhodoliths at the different regions. Percentage of large (d), medium (e) and small (f) rhodoliths with respect to the sum of BW and PR at the different regions. Percentage of PR with encrusting-warty (g), lumpy (h) and fruticose (i) growth form with respect to the total number of pralines at the different regions. (PO-PA: saddle between Palmarola and Ponza; NE PA: region off the NE of Palmarola; NW PA: region of the NW of Palmarola; PO ZA: saddle between Ponza and Zannone; N ZA: region of the N of Zannone).

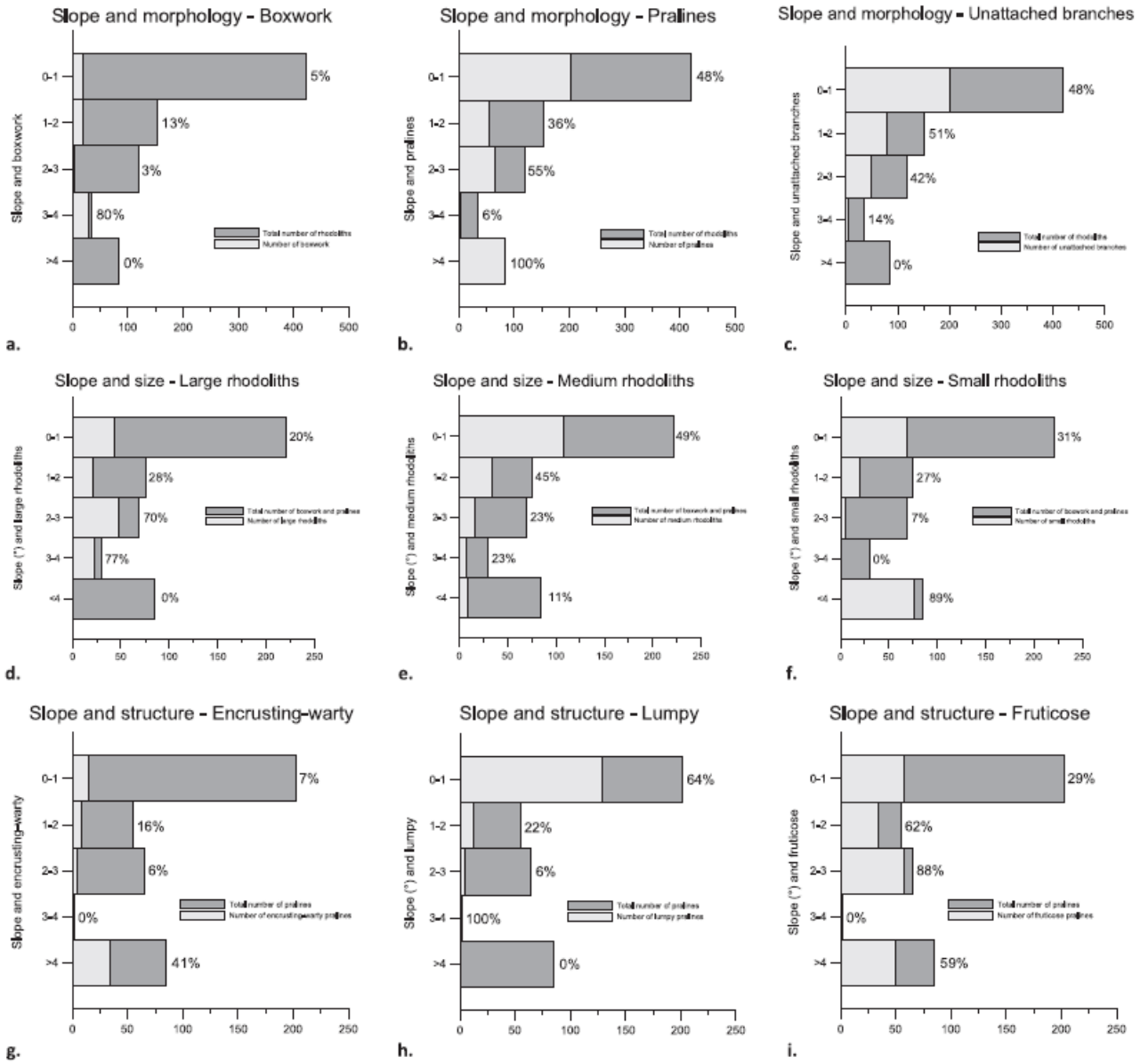

Fig. 8. Effects of the bottom slope on rhodolith morphology, size and growth form. Percentage of BW (a), PR (b) and BR (c) with respect to the total number of rhodoliths at different slopes. Percentage of large (d), medium (e) and small (f) rhodoliths with respect to the sum of BW and PR at different slopes. Percentage of PR with encrusting-warty (g), lumpy (h) and fruticose (i) growth form with respect to the total number of PR at different slopes.

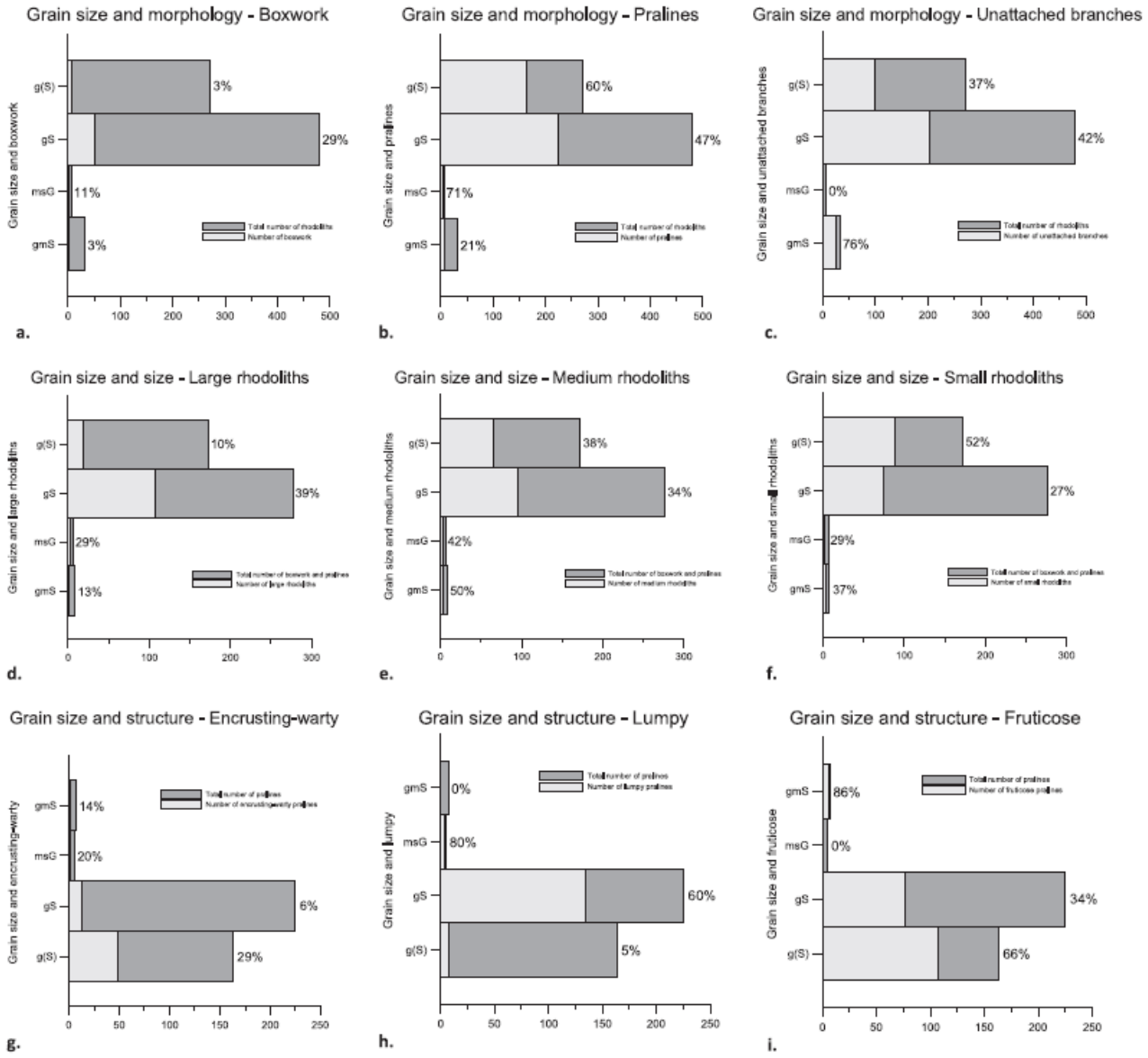

Fig. 9. Effects of sediment grain size on rhodolith morphology, size and growth form. Percentage of BW (a), PR (b), and BR (c) with respect to the total number of rhodoliths corresponding at different sediment grain size. Percentage of large (d), medium (e) and small (f) rhodoliths with respect to the sum of BW and PR corresponding at different sediment grain size. Percentage of PR with encrusting-warty (g), lumpy (h) and fruticose (i) growth form with respect to the total number of PR corresponding at different sediment grain size. ((g)S: slightly gravelly sand; gS: gravelly sand; msG: muddy sandy gravel; gmS: gravelly muddy sand).

Table 1

Description of the 27 grabs with living rhodoliths including the algal species (*Lithothamnion valens, Lithothamnion minervae, Lithophyllum racemus, Spongites fruticulosus, Phymatolithon calcareum*) forming the nodules.

Grab	Lat.	Long.	Depth (m)	Region	Slope (deg)	Grain size	Rhod. (no)	Rhodoliths morphology			Size			Prälines structure			Rhodolith-forming species					
								BW	PR	BR	Large	Medium	Small	EW	L.	F	Lv	Lm	Lr	Sf	Pc
PO-PA1	324115	4527289	72	PO-PA	0.9	(g)S	102	0	62	40	8	44	10	0	7	55					
PO-PA2	322934	4528534	76	PO-PA	0.2	(g)S	1	1	0	0	1	0	0	0	0	0			x	x	
PO-PA3	324256	4527973	71	PO-PA	0.8	gS	36	10	19	7	13	16	0	11	8	0					
PO-PA4	322512	4531008	70	PO-PA	1.2	(g)S	10	0	5	5	0	5	0	0	5	0					
PO-PA5	323079	4531409	75	PO-PA	5.2	(g)S	85	0	85	0	0	9	76	0	35	50					
PO-PA6	324068	4528763	70	PO-PA	1.5	(g)S	3	0	0	3				0	0	0	x				
PO-PA7	324904	4530740	59	PO-PA	2.9	gS	4	3	0	1	1	1	1	0	0	0			x		
PO-PA8	325637	4531135	60	PO-PA	3.5	gS	2	0	2	0	2	0	0	2	0	0			x	x	
PO-PA9			61	PO-PA	1.75		22	8	8	6	7	7	2	0	0	8					
PO-PA10	318503	4529704	79	PO-PA	1	(g)S	52	0	3	49	0	3	0	0	0	3					
NW PA1	320275	4537628	88	NW PA	1.4	(g)S	8	6	0	2	6	0	0	0	0	0					
NW PA2	319710	4536768	70	NW PA	0.7	gS	281	8	121	152	22	48	59	118	0	3		x	x		x
NW PA3	319135	4536184	43	NW PA	1.1	gS	6	0	6	0	1	1	4	0	0	6					
PO-PA11	317371	4532692	56	PO-PA	1.5	msG	7	2	5	0	2	3	2	4	1	0	x		x		
PO-PA12	316071	4530796	68	PO-PA	1.4	(g)S	7	0	7	0	3	1	3	7	0	0				x	
PO-PA13	314818	4532285	58	PO-PA	0.8	gS	1	0	0	1				0	0	0	x			x	
NW PA4	317906	4534918	61	NW PA	1.5	gS	19	4	11	4	2	4	9	1	1	9		x		x	
PO-ZA1	334133	4534518	59	PO-ZA	2	gS	11	0	1	10	0	1	0	0	0	1					
N ZA1	335559	4537872	57	N ZA	2.2	gS	16	0	0	16				0	0	0	x				
N ZA2	337605	4538401	45	N ZA	2.2	gmS	27	0	6	21	0	3	3	0	0	6		x			
PO-ZA2	330365	4534368	63	PO-ZA	1.1	gmS	5	0	1	4	0	1	0	0	1	0			x		
N ZA3	338140	4538633	64	E ZA	1.3	gS	14	0	9	5	0	9	0	0	1	8					
PO-ZA3			53	PO-ZA	2.5	gS	58	0	56	2	46	9	1	3	3	50				x	
PO-ZA4	333200	4536790	90	PO-ZA	3.4	gS	32	27	0	5	21	6	0	0	0	0					
PO-ZA5	332090	4536717	112	PO-ZA	2.4	gmS	1	1	0	0	1	0	0	0	0	0					
PO-PA14	323443	4529610	64	PO-PA	3.5	(g)S	1	1	0	0	0	1	0	0	0	0	x				
PO-PA15	325537	4527362	74	PO-PA	2.1	(g)S	2	0	2	0	0	2	0	1	1	0			x		

Abbreviations: **PO**: Ponza Island; **PA**: Palmarola Island; **ZA**: Zannone Island; **PO-PA**: saddle between Ponza and Palmarola; **PO-ZA**: saddle between Ponza andZannone; **(g)S**: slightly gravelly sand; **gS**: gravelly sand; **msG**: muddy sandy gravel; **gmS**: gravelly muddy sand; **B**: boxwork; **P**: pralines; **UB**:unattached branches; **EW**: encrusting-warty; **L**: lumpy; **F**: fruticose; **Lv**: *Lithothamnion valens*; **Lm**: *Lithothamnion minervae*; **Lr**: *Lithophyllum racemus*; **Sf**: *Spongites fruticulosus*; **Pc**: *Phymatolithon calcareum*.

Table 2

Description of the 8 sonar facies where rhodoliths were sampled.

Facies name	**Low backscatter (LB)**	**Low backscatter disomogeneous (D-LB)**	**High backscatter (HB)**	**High backscatter disomogeneous (D-HB)**	**Rocks-high backscatter (r-HB)**	***Posidonia oceanica* (POS)**
Description	Fine sediment	Alternation of high and low backscatter. Prevalence of low backscatter areas.	Coarse bioclastic sediment with abundant rhodoliths.	Alternation of high and low backscatter. Prevalence of high backscatter areas.	Rocks surrounded by high backscatter.	Typical sonar facies of *Posidonia oceanica* meadows.

Table 3

Description of the 21 ROV videos were rhodoliths were observed.

ROV video	Latitude	Longitude	Description
R1	315853	4530815	Megaripples
R2	319657	4536273	Megaripples
R3	316818	4536799	Megaripples
R4	315733	4536020	Megaripples
R5	317915	4534905	Megaripples
R6	324425	4526805	Rocks
R7	323246	4527611	Megaripples
R8	323017	4528175	Flat bottom
R9	319694	4527925	Rocks
R10	323059	4531450	Flat bottom
R11	323355	4529650	Megaripples
R12	321523	4530745	Flat bottom
R13	319796	4528171	Rocks
R14	319709	4527241	Rocks
R15	340562	4538937	Flat bottom
R16	343378	4539243	Rocks
R17	343430	4539557	Flat bottom
R18	340297	4537643	Rocks
R19	337167	4538039	Megaripples
R20	338471	4538112	Megaripples
R21	334581	4539152	Rocks

Table 4

Results of the univariate (a) and multivariate (b and c) statistical tests. Significant differences are in bold. Results of the univariate statistical test ANOVA for the abundance of rhodoliths and depth (0–40 m, 40–60 m, 60–80 m, 80–110 m and > 110 m), region (E islands, saddle, NW PA, NE PA, N ZA and BOTTE), slope (0–2°, 2–3°, 3–4° and > 4°) and grain size (gravel, sand and mud) for all grabs (a). Results of the multivariate statistical test ANOSIM for rhodoliths morphology, size and growth form, and the four environmental variables: depth (40-60 m, 60–80 m and 80–110 m), region (saddle, NW PA and NW ZA), slope (0–2°, 2–3°, 3–4° and > 4°) and grain size ((g)S + gS, msG and gmS) (b). Results of the multivariate statistical test ANOSIM separately for rhodoliths morphology, size and structure, and the four environmental variables: depth (40-60 m, 60-80 m and 80-110 m), region (saddle, NW PA and NW ZA), slope (0–2°, 2–3°, 3–4° and > 4°) and grain size ((g)S + gS, msG and gmS) (c).

"SS" means "Sum of Squares".
"DF" means "Degrees of Freedom".
"MS" means "Mean Squares" and is obtained dividing the sum of squares by the degrees of freedom.
"F" represents the result of the F-Test and is obtained dividing the mean squares of the inter-group variability by the mean squares of the intra-group variability.

Variable	Environmental parameter	Variability	SS	DF	MS	F	p-level
Abundance	Depth	Effect	2129.733	4	532.433	0.956	0.433
		Error	98555.13	177	556.809		
	Region	**Effect**	**26600.68**	**5**	**5320.137**	**12.639**	**0.000**
		Error	**74084.18**	**176**	**420.933**		
	Slope	Effect	923.638	3	307.880	0.549	0.649
		Error	99761.22	178	560.456		
	Grain size	Effect	171.556	2	85.778	0.153	0.859
		Error	100513.3	179	561.527		

(a)

Variable	Environmental parameter	Global R	P
Morphology, size, structure	**Depth**	**0.9**	**0.02**
	Region	0.56	0.3
	Slope	1	0.1
	Grainsize	0.2	0.5

(b)

Environmental parameter	Variable		
	MORPHOLOGY	SIZE	GROWTH FORM
Depth	**R=0.75; P=0.03**	**R=0.65; P=0.06**	**R=0.95; P=0.01**
Region	R=0.56; P=0.30	R=-0.56; P=0.80	R=0.33; P=0.40
Slope	R=0.78; P=0.20	R=0.10; P=0.10	R=0.11; P=0.50
Grainsize	R=1.00; P=0.17	R=−1.00; P=1.00	R=0.20; P=0.50

(c)